Physics Letters B 827 (2022) 137006

Contents lists available at ScienceDirect

Physics Letters B

www.elsevier.com/locate/physletb

First observation of the coexistence of multiple chiral doublet bands and pseudospin doublet bands in the $A \approx 80$ mass region

L. Mu [a], S.Y. Wang [a,*], C. Liu [a], B. Qi [a], R.A. Bark [b], J. Meng [c,d,e], S.Q. Zhang [c], P. Jones [b], S.M. Wyngaardt [e], H. Jia [a], Q.B. Chen [f], Z.Q. Li [a], S. Wang [a], D.P. Sun [a], R.J. Guo [a], X.C. Han [a], W.Z. Xu [a], X. Xiao [a], P.Y. Zhu [a], H.W. Li [a], H. Hua [c], X.Q. Li [c], C.G. Li [c], R. Han [c], B.H. Sun [g], L.H. Zhu [g], T.D. Bucher [b,e], B.V. Kheswa [b,e], N. Khumalo [b,h,i], E.A. Lawrie [b,h], J.J. Lawrie [b], K.L. Malatji [b,e], L. Msebi [b,h], J. Ndayishimye [b,e], J.F. Sharpey-Schafer [h], O. Shirinda [b,e], M. Wiedeking [b,j], T. Dinoko [k], S.S. Ntshangase [i]

[a] Shandong Provincial Key Laboratory of Optical Astronomy and Solar-Terrestrial Environment, School of Space Science and Physics, Institute of Space Sciences, Shandong University, Weihai 264209, People's Republic of China
[b] iThemba LABS, 7129 Somerset West, South Africa
[c] State Key Laboratory of Nuclear Physics and Technology, School of Physics, Peking University, Beijing 100871, People's Republic of China
[d] Yukawa Institute for Theoretical Physics, Kyoto University, Kyoto 606-8502, Japan
[e] Department of Physics, University of Stellenbosch, Matieland 7602, South Africa
[f] Department of Physics, East China Normal University, Shanghai 200241, People's Republic of China
[g] School of Physics, Beihang University, Beijing 100191, People's Republic of China
[h] Department of Physics, University of the Western Cape, P/B X17, Bellville 7535, South Africa
[i] Department of Physics, University of Zululand, Private Bag X1001, KwaDlangezwa 3886, South Africa
[j] School of Physics, University of the Witwatersrand, Johannesburg 2050, South Africa
[k] National Metrology Institute of South Africa, DCLF-RF, Private Bag X34, Lynnwood Ridge, Pretoria 0040, South Africa

ARTICLE INFO

Article history:
Received 29 March 2021
Received in revised form 14 January 2022
Accepted 28 February 2022
Available online 4 March 2022
Editor: B. Blank

Keywords:
High-spin states
Chiral doublet bands
Pseudospin doublet
Covariant density functional theory
Particle rotor model
^{81}Kr

ABSTRACT

Two nearly degenerate positive-parity bands with the $\pi g_{9/2}^2 \otimes \nu g_{9/2}^{-1}$ configuration and three nearly degenerate negative-parity bands with the $\pi g_{9/2}(p_{3/2}, f_{5/2}) \otimes \nu g_{9/2}^{-1}$ configuration have been identified in ^{81}Kr. They are interpreted as chiral doublet bands and pseudospin-chiral triplet bands, which is supported by the constrained covariant density functional theory and the multiparticle plus rotor model calculations. The present work reports two new chiral configurations $\pi g_{9/2}^2 \otimes \nu g_{9/2}^{-1}$ and $\pi g_{9/2}(p_{3/2}, f_{5/2}) \otimes \nu g_{9/2}^{-1}$, and the first example of pseudospin-chiral triplet bands involving the $\pi(p_{3/2}, f_{5/2})$ pseudospin doublet.

© 2022 The Author(s). Published by Elsevier B.V. This is an open access article under the CC BY license (http://creativecommons.org/licenses/by/4.0/). Funded by SCOAP[3].

1. Introduction

Chirality is a common property in nature. Well-known examples of systems demonstrating chirality are found in chemistry, biology, particle physics, etc. In nuclear physics, chirality was first predicted by Frauendorf and Meng in 1997 [1]. They pointed out that chirality is expected to occur in triaxial nuclei with unpaired particle(s) and hole(s) in high-j orbitals. The experimental signal for chiral symmetry breaking in atomic nuclei is the existence of two nearly degenerate $\Delta I = 1$ bands with the same parity, which are called chiral doublet bands. Since then, much effort has been devoted to searching for such bands in experiments. So far, candidates for chiral doublet bands have been reported in about 50 nuclei in the $A \approx 80$, 100, 130, and 190 mass regions (see recent reviews [2–7] and references therein).

In 2006, based on the constrained triaxial covariant density functional theory (CDFT) calculations, Ref. [8] suggested that multiple chiral doublet bands (MχD) can exist in a single nucleus. In 2013, two distinct sets of chiral doublet bands were identified in ^{133}Ce [9], which was regarded as the first strong experimen-

* Corresponding author.
E-mail address: sywang@sdu.edu.cn (S.Y. Wang).

https://doi.org/10.1016/j.physletb.2022.137006
0370-2693/© 2022 The Author(s). Published by Elsevier B.V. This is an open access article under the CC BY license (http://creativecommons.org/licenses/by/4.0/). Funded by SCOAP[3].

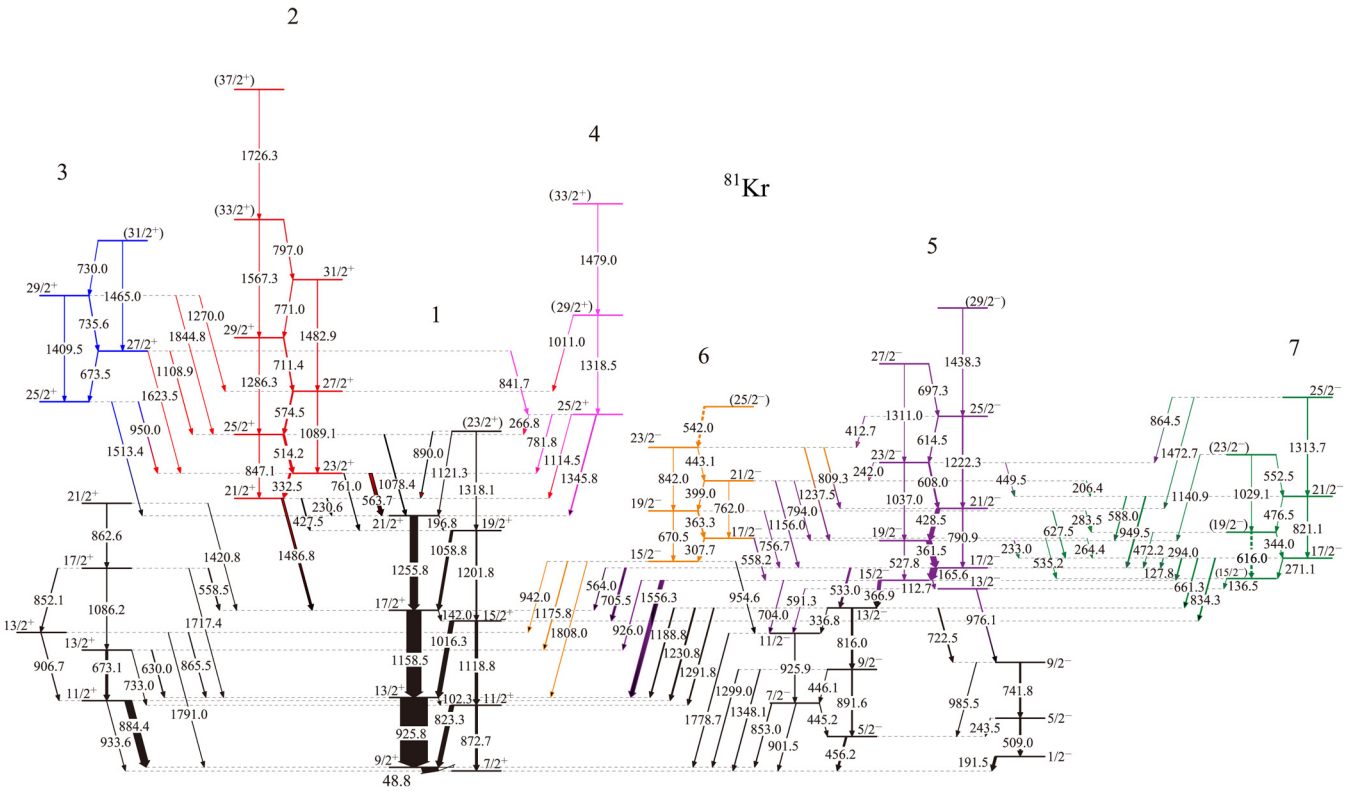

Fig. 1. Level scheme of ^{81}Kr derived from the present work. The energies are given in keV, and the widths of the arrows are proportional to the relative transition intensities. Levels and intraband transitions are colored in group by bands. The ends of linking transitions are colored by their initial states while the tips are colored by their final states.

tal evidence for the existence of MχD. Subsequently, the study of MχD has become a hot topic in nuclear physics and a series of experiments were performed to further explore this interesting phenomenon. Until now, MχD have been reported in several nuclei [10,11], i.e., ^{133}Ce [9], ^{103}Rh [12], ^{78}Br [13], ^{136}Nd [14], ^{195}Tl [15], ^{135}Nd [16], ^{131}Ba [17], ^{137}Nd [18] and possibly in ^{107}Ag [19].

In 2016, the MχD with octupole correlations were identified in odd-odd ^{78}Br [13], which indicates that a simultaneous breaking of chirality and reflection symmetries may exist in nuclei. It motivates further studies of the coexistence of multiple symmetries in a single nucleus [20,21]. Recently, the coexistence of chiral symmetry and pseudospin symmetry has attracted significant attention. More introduction on pseudospin symmetry can be seen in Refs. [22,23]. A specific calculation [24] for the three nearly degenerate bands with the $\pi g_{9/2}^{-1} \otimes \nu h_{11/2}(d_{5/2}, g_{7/2})$ configuration in ^{105}Ag was performed by using the CDFT and the multiparticle plus rotor model (MPRM), which suggested that the 1st and 2nd, and, the 2nd and 3rd lowest energy bands were the pseudospin doublet bands and chiral doublet bands, respectively, thereby forming a set of pseudospin-chiral triplet bands [24]. It points to the possibility of pseudospin-chiral quartet bands existing in atomic nuclei. Very recently, Ref. [17] claimed that such quartet bands with the $\pi h_{11/2}(d_{5/2}, g_{7/2}) \otimes \nu h_{11/2}$ configuration have been observed in ^{131}Ba. It is worth noting that the pseudospin-chiral triplet and quartet bands mentioned above both involve the $(d_{5/2}, g_{7/2})$ pseudospin doublet. Thus, it is of highly scientific interest to investigate whether pseudospin doublets based on other configurations are also suitable for the construction of pseudospin-chiral triplet (or quartet) bands.

In the $A \approx 100$, 130 and 190 mass regions, chirality manifests itself not only in the odd-odd systems but also in odd-A or even-even systems. However, the $A \approx 80$ mass region is a relatively new territory of chirality with four cases of odd-odd nuclei, namely ^{78}Br [13], ^{80}Br [25], ^{82}Br [26] and ^{84}Rb [27]. Thus, it is interesting to search for chiral doublet bands (or MχD) in odd-A or even-even nuclei in the $A \approx 80$ mass region. Additionally, pseudospin doublet bands are also expected to coexist with chiral doublet bands (or MχD) in this mass region since the quasi-particles may occupy the pseudospin partner orbitals $p_{3/2}$ and $f_{5/2}$.

In this Letter, by investigating the medium- and high-spin states in the odd-A nucleus ^{81}Kr, we find two new chiral configurations $\pi g_{9/2}^2 \otimes \nu g_{9/2}^{-1}$ and $\pi g_{9/2}(p_{3/2}, f_{5/2}) \otimes \nu g_{9/2}^{-1}$, and the first example of pseudospin-chiral triplet bands involving the $\pi(p_{3/2}, f_{5/2})$ pseudospin doublet.

2. Experiment

Medium- and high-spin states in the odd-A nucleus ^{81}Kr were populated via the strongest channel of the fusion evaporation reaction α + ^{82}Se at beam energies of 65 and 68 MeV. The target consisted of a 0.36 mg/cm^2 ^{82}Se foil with 0.01 mg/cm^2 ^{12}C backing. The emitted γ-rays were detected by the AFRODITE array [28], which comprised eight Compton-suppressed clover detectors. A total of approximately 1.45×10^9 two-fold coincidence events were accumulated. The level scheme of ^{81}Kr was constructed using γ-γ coincidence relations and relative intensities of the γ transitions. Spin and parity assignments were made on the basis of the measurements of the angular distributions from the oriented states (ADO) [29] and the polarization asymmetry (A_p) [30]. As by-products of this experiment, excited states of ^{82}Br and ^{79}Se were studied and reported in Refs. [26,31]. More details of the experimental setup and procedure can be found in Refs. [26,31].

3. Results and discussions

The level scheme of ^{81}Kr derived from the present work is shown in Fig. 1. As shown in Fig. 1, the observed transitions are

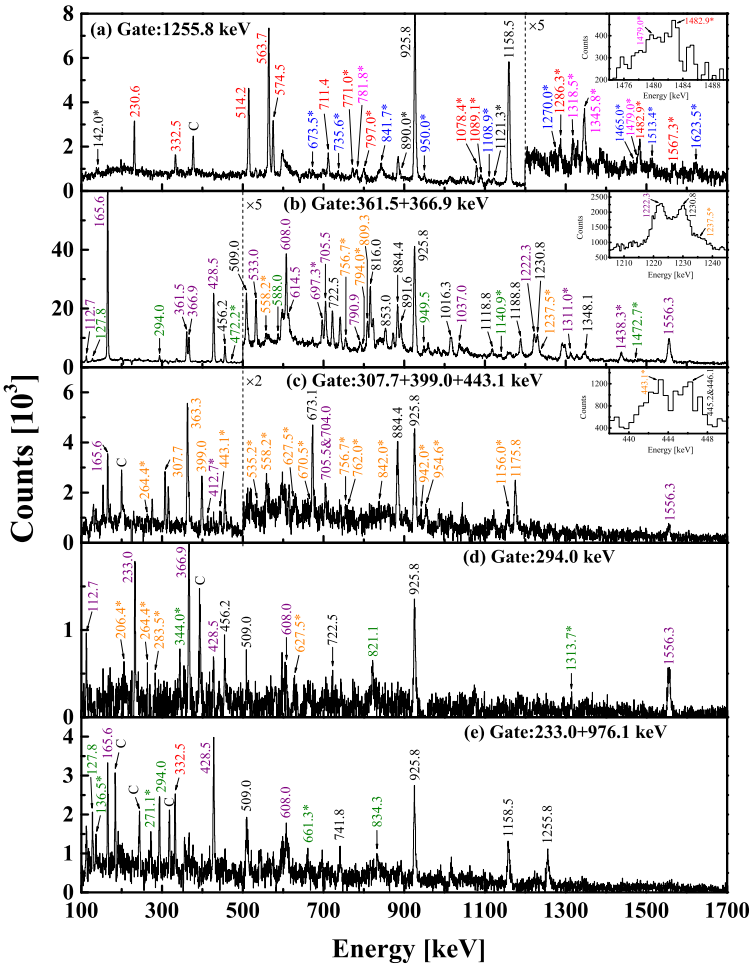

Fig. 2. The γ-γ coincidence spectra gated on the (a) 1255.8 keV ($21/2^+ \rightarrow 17/2^+$) transition of band 1 (b) 361.5 keV ($19/2^- \rightarrow 17/2^-$) + 366.9 keV ($15/2^- \rightarrow 13/2^-$) transitions of band 5 (c) 307.7 keV ($17/2^- \rightarrow 15/2^-$) + 399.0 keV ($21/2^- \rightarrow 19/2^-$) + 443.1 keV ($23/2^- \rightarrow 21/2^-$) transitions of band 6 (d) 294.0 keV ($17/2^- \rightarrow 15/2^-$) transition of band 7 (e) 233.0 keV ($19/2^- \rightarrow 17/2^-$) + 976.1 keV ($13/2^- \rightarrow 9/2^-$) transitions of band 5 in ^{81}Kr. The insets in spectra (a), (b) and (c) show the expanded regions around 1479.0, 1237.5 and 443.1 keV, respectively. The newly identified transitions are marked with an asterisk. The peaks labeled C indicate contaminations. The peak energies are colored by the initial state of γ-rays.

roughly grouped into seven bands labeled as 1−7, of which bands 1, 2, 5 and 6 were known previously [32,33]. Fig. 2 presents sample spectra to show the γ-γ coincidence relations in ^{81}Kr. For the positive-parity part, bands 1 and 2 have been extended from $21/2^+$ and $(29/2^+)$ to $(23/2^+)$ and $(37/2^+)$, respectively, bands 3 and 4 are newly identified. The new transitions in bands 2, 3 and 4 can be seen in Fig. 2(a). For the negative-parity part, the present work extends bands 5 and 6 from $(25/2^-)$ and (21/2) to $(29/2^-)$ and $(25/2^-)$, respectively. Fig. 2(b) shows the newly identified intraband transitions of band 5 and interband transitions which feed into band 5. Fig. 2(c) shows the intraband transitions of band 6 and the interband transitions deexcited out of band 6. It is worth mentioning that band 7 is newly observed in the present work, and most of its transitions can be seen in Figs. 2(d) and (e).

Prior to this work, bands 1, 2 and 5 had already been assigned spins and parities, however, only tentative spin assignments were given for band 6 [33]. On the basis of the measured ADO ratios and A_p values, the present work confirms the previous known spin-parity assignments and assigns the spins and parities for the newly observed levels. Fig. 3 provides the extracted ADO ratios and A_p values for the selected linking transitions in ^{81}Kr. For example, as shown in Fig. 3, the ADO ratio and the A_p value of the 950.0 keV transition between the lowest observed state of band 3 and the $23/2^+$ state of band 2 are 1.03(0.14) and −0.11(0.08), respectively. These values suggest that the 950.0 keV linking transition has an $M1/E2$ character. Thus, we assign the spin and parity $25/2^+$ for the lowest observed state of band 3. The similar analyses lead to the current spin-parity assignments shown in Fig. 1.

To study the properties of the rotational bands in ^{81}Kr, the quasiparticle alignments i_x for all bands were extracted and presented in Fig. 4. The excitation energies $E(I)$ and the reduced transition probability ratios $B(M1)/B(E2)$ for bands 2, 3, 5, 6 and 7 were also extracted and presented in Fig. 5. Bands 1 and 2 have been already assigned the $\nu g_{9/2}^{-1}$ and $\pi g_{9/2}^2 \otimes \nu g_{9/2}^{-1}$ configurations, respectively [32,33]. The existence of several $M1/E2$ and $E2$ linking transitions between bands 2 and 3 implies that band 3 has the same intrinsic configuration $\pi g_{9/2}^2 \otimes \nu g_{9/2}^{-1}$ as band 2, as argued in Refs. [34–36]. As seen from Fig. 4, the i_x values of band 3 are close to those of band 2, which further supports the present configuration assignment for band 3. As shown in Figs. 5(a1) and 5(a2), the $E(I)$ for bands 2 and 3 are close to each other, the $B(M1)/B(E2)$ for both bands are similar and show odd-even staggering with the same phase as a function of spin. These behaviors are consistent with the fingerprints of chiral doublet bands [2,37–39]. Thus, bands 2 and 3 are likely to be a pair of chiral doublet bands.

In the $A \approx 80$ mass region, the $g_{9/2}$ proton and neutron alignments were suggested to take place at $\hbar\omega \approx 0.4-0.5$ and $0.6-0.7$ MeV, respectively [40,41]. As shown in Fig. 4, band 2 crosses band 1 at $\hbar\omega \approx 0.5$ MeV, while band 4 crosses band 1 at a higher frequency of $\hbar\omega \approx 0.65$ MeV. The band crossing between bands 1

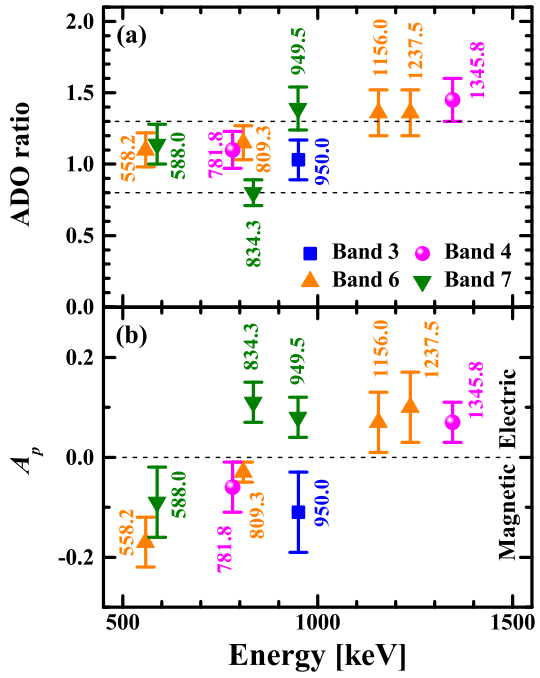

Fig. 3. The ADO ratios (a) and the A_p values (b) for the select linking transitions in ^{81}Kr. In the present work, ADO ratios ≈1.3 and ≈0.8 (correspond to the dashed lines in the upper panel) are expected for the stretched quadrupole and pure stretched dipole transitions, respectively [26]. The transition energies are colored by the initial state of γ-rays. In the lower panel, the positive and negative values correspond to the electric and magnetic transitions, respectively.

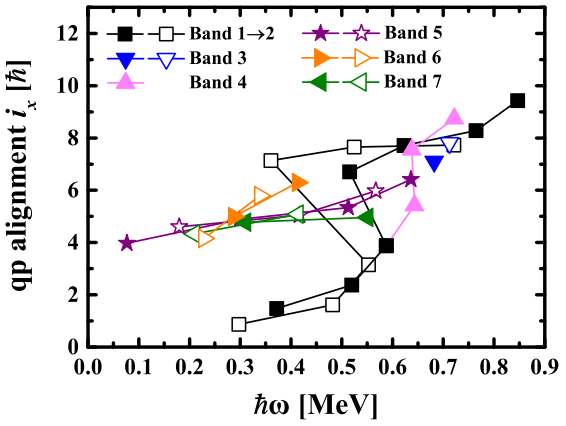

Fig. 4. Quasiparticle alignments i_x as function of rotational frequency for all bands in ^{81}Kr. Colors of experimental points are consistent with Fig. 1. The solid and open symbols correspond to the branches with spin $I = 2n + 1/2$ and $2n - 1/2$ ($n = 1, 2...$), respectively. The Harris parameters used are $\mathcal{J}_0 = 9.0\ \hbar^2$/MeV and $\mathcal{J}_1 = 1.0\ \hbar^4$/MeV^3.

and 2 occurs in the frequency range of the $g_{9/2}$ proton alignment, which is consistent with the previous configuration assignments [32,33]. On the other hand, the band crossing between bands 1 and 4 occurs in the frequency range of the $g_{9/2}$ neutron alignment. Consequently, band 4 is assigned the $\nu g_{9/2}^{-3}$ configuration. The CDFT calculation for band 4 in the present work shows that band 4 has an oblate shape with a quadrupole deformation ($\beta = 0.27$, $\gamma = 60.0°$). In the case of such deformation, the valence neutrons in ^{81}Kr occupy the high-j low-Ω orbitals. This will result in a large signature splitting and so that one signature sequence is not easily to be observed, which is consistent with the observation of band 4 in this experiment.

In Ref. [33], bands 5 and 6 were assigned the $\pi g_{9/2}(p_{3/2}, f_{5/2}) \otimes \nu g_{9/2}^{-1}$ configuration. Similar to the above analysis on bands 2 and 3, based on the similar i_x values (see Fig. 4) and the existence of $M1/E2$ and $E2$ linking transitions (see Fig. 1), bands 5, 6 and 7 are considered to have the same $\pi g_{9/2}(p_{3/2}, f_{5/2}) \otimes \nu g_{9/2}^{-1}$ configuration. As shown in Figs. 5(b1) and 5(b2), bands 5 and 6 exhibited the expected properties of chiral doublet bands, i.e., the close $E(I)$, the similar $B(M1)/B(E2)$, and the same phase in the $B(M1)/B(E2)$ staggering. However, as shown in Fig. 5(c2), bands 5 and 7 show the opposite phase in the $B(M1)/B(E2)$ staggering, which is consistent with the characteristic of pseudospin doublet bands proposed in Refs. [23,42]. Therefore, bands 6 and 7 are suggested as the chiral partner and the pseudospin partner of band 5, respectively. It is worth mentioning that the $\pi g_{9/2}p_{3/2} \otimes \nu g_{9/2}^{-1}$ and $\pi g_{9/2}f_{5/2} \otimes \nu g_{9/2}^{-1}$ configurations have different favored signature branches. From the signature argument, the largest component of the configuration for band 5 would be $\pi g_{9/2}p_{3/2} \otimes \nu g_{9/2}^{-1}$. Thus, for the chiral partner (band 6) and the pseudospin partner (band 7) of band 5, the largest components of their configurations may be proposed as $\pi g_{9/2}p_{3/2} \otimes \nu g_{9/2}^{-1}$ and $\pi g_{9/2}f_{5/2} \otimes \nu g_{9/2}^{-1}$, respectively.

To further investigate the nature of the nearly degenerate bands 2 and 3 as well as bands 5, 6 and 7, we carried out the calculations based on the constrained triaxial CDFT [8,43–45] and the MPRM [46,47]. The CDFT calculations with the parameter set PK1 [48] show that the bandheads of the $\pi g_{9/2}^2 \otimes \nu g_{9/2}^{-1}$ and $\pi g_{9/2}(p_{3/2}, f_{5/2}) \otimes \nu g_{9/2}^{-1}$ configurations have triaxial shapes with the deformation parameters $(\beta, \gamma) = (0.28, 45.4°)$ and $(0.24, 43.3°)$, respectively. Subsequently, the quadrupole deformation parameters β obtained from the CDFT calculations were used as inputs to the MPRM calculations, while the triaxial deformation parameters γ were adjusted since the values of γ usually vary as rotational frequency increasing [24,49–51]. The values of $\gamma = 24.0°$ ($31.0°$) were used for bands 2 and 3 (bands 5, 6 and 7), which were adjusted to obtain the best agreement between the theoretical calculations and the experimental data. Taking the effect of the strong mixing between low-j protons into account, a Coriolis attenuation factor of $\xi = 0.85$ has been employed for bands 5, 6 and 7. The other parameters in MPRM follow Refs. [46,47,52].

The $E(I)$ and $B(M1)/B(E2)$ calculated by the MPRM for bands 2 and 3 with the $\pi g_{9/2}^2 \otimes \nu g_{9/2}^{-1}$ configuration, bands 5 and 6 with the $\pi g_{9/2}p_{3/2} \otimes \nu g_{9/2}^{-1}$ configuration, and band 7 with the $\pi g_{9/2}f_{5/2} \otimes \nu g_{9/2}^{-1}$ configuration are shown in Fig. 5, in comparison with the available data. As shown in Figs. 5(a1) and 5(a2), the MPRM calculations for bands 2 and 3 are in good agreement with the experimental data except for the $B(M1)/B(E2)$ at low spin. In Figs. 5(b1) and 5(c1), the calculated $E(I)$ for bands 5, 6 and 7 reproduce the characteristic of energy degeneracy observed experimentally. In addition, in Figs. 5(b2) and 5(c2), the calculated results show that the staggering phase of $B(M1)/B(E2)$ in band 5 is the same as band 6, but opposite to band 7, which reproduce the experimental staggering and the trend pattern well. The agreement between the calculated values and the corresponding experimental data provides additional support for the present configuration assignments and interpretations of the observed bands.

To examine the angular momentum geometry for the nearly degenerate bands 2 and 3 as well as bands 5, 6 and 7 in ^{81}Kr, the *azimuthal plots* [53–61], i.e., probability density profiles $\mathcal{P}(\theta, \phi)$ for the orientation of the angular momentum on the (θ, ϕ) plane, are calculated and plotted in Figs. 6 and 7. Here, the θ is the angle between the total spin $\boldsymbol{I}$ and the long-axis (l-axis), and the ϕ is the angle between the projection of $\boldsymbol{I}$ onto the intermediate-short (i-s) plane and the i-axis. Details of the calculation process can be seen in Refs. [53,56].

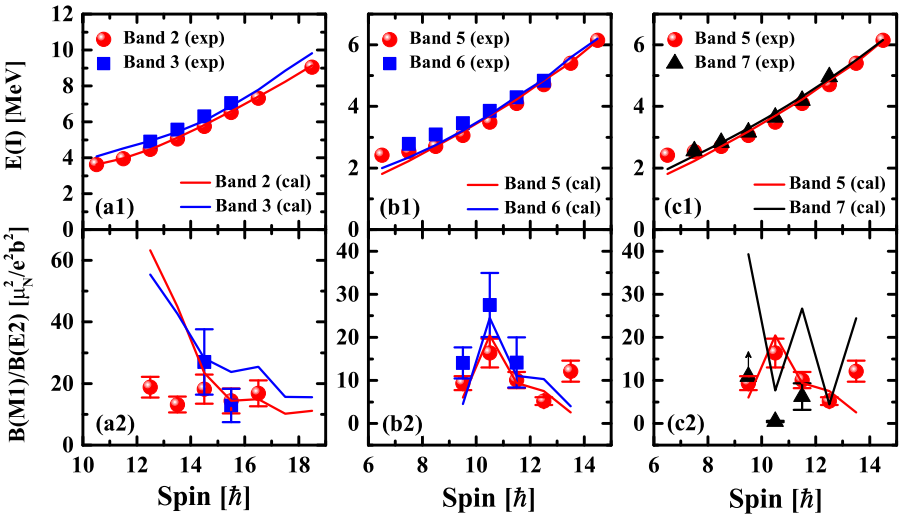

Fig. 5. The experimental $E(I)$ and $B(M1)/B(E2)$ for bands 2, 3 with the $\pi g_{9/2}^2 \otimes \nu g_{9/2}^{-1}$ configuration and bands 5, 6, 7 with the $\pi g_{9/2}(p_{3/2}, f_{5/2}) \otimes \nu g_{9/2}^{-1}$ configuration in ^{81}Kr in comparison with the MPRM results. The energies at $I = 25/2\hbar$, $I = 17/2\hbar$ and $I = 17/2\hbar$ are taken as references for bands 2, 5 and 7, respectively.

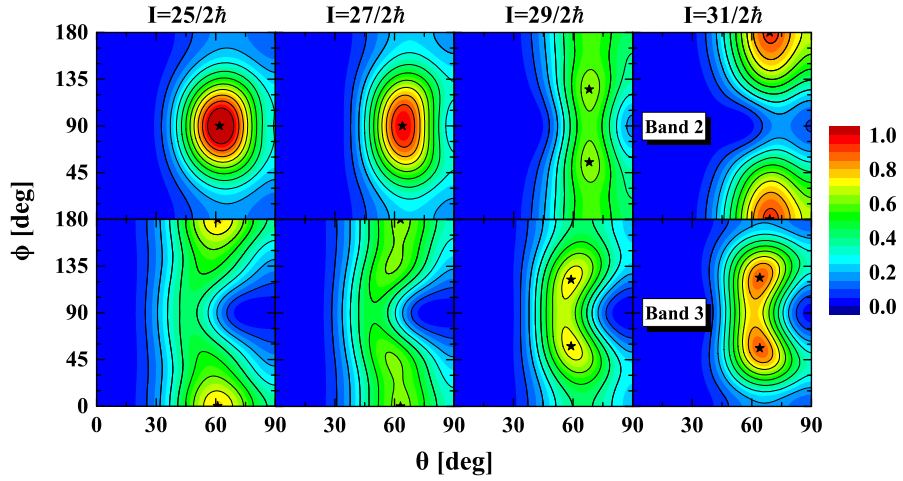

Fig. 6. The *azimuthal plots* calculated for bands 2 and 3 at $I = 25/2\hbar$, $27/2\hbar$, $29/2\hbar$ and $31/2\hbar$. The black star represents the position of a local maximum.

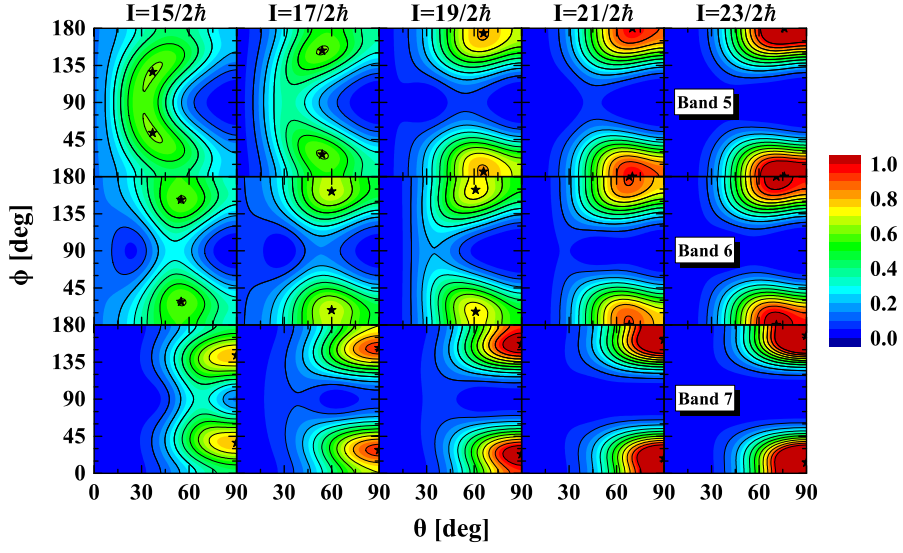

Fig. 7. Same as Fig. 6, but calculated for bands 5, 6 and 7 at $I = 15/2\hbar$, $17/2\hbar$, $19/2\hbar$, $21/2\hbar$ and $23/2\hbar$.

Fig. 6 shows the *azimuthal plots* for bands 2 and 3 at $I = 25/2$, $27/2$, $29/2$ and $31/2\hbar$. At $I = 25/2$ and $27/2\hbar$, the *azimuthal plots* for band 2 have only one single peak at ($\theta \approx 60°$, $\phi \approx 90°$). The angle $\phi \approx 90°$ indicates that the orientation of the angular momentum is perpendicular to the i-axis. Thus, the angular momentum for band 2 stays within the s-l plane, which corresponds to a planar rotation. The *azimuthal plots* for band 3 have two peaks at ($\theta \approx 60°$, $\phi \approx 0°$) and ($\theta \approx 60°$, $\phi \approx 180°$), namely, a planar rotation within the i-l plane. At $I = 29/2\hbar$, the *azimuthal plots* for bands 2 and 3 are similar, with two peaks at (68°, 55°) and (68°, 125°) for band 2, and (59°, 58°) and (59°, 122°) for band 3. This shows a picture of nearly static chirality. At $I = 31/2\hbar$, the angular momenta for band 2 orientate at (69°, 0°) and (69°, 180°), corresponding to an i-l planar rotation. The angular momenta for band 3 orientate at (64°, 56°) and (64°, 124°), corresponding to an aplanar rotation. These orientations are in accordance with the interpretation of chiral vibration, as discussed in Refs. [53–55,57–59,61]. Therefore, as the spin increases, the rotational modes of bands 2 and 3 change from the planar rotations to the nearly static chirality and then to the chiral vibration.

A similar analysis also applies to bands 5, 6 and 7. Fig. 7 shows their *azimuthal plots* at $I = 15/2$, $17/2$, $19/2$, $21/2$ and $23/2\hbar$. One can see in Fig. 7 that bands 5 and 6 exhibit the evolutions of rotational modes from the nearly static chirality at $I = 15/2$, $17/2\hbar$, then to the chiral vibration at $I = 19/2\hbar$, and finally to the planar rotations at $I = 21/2$, $23/2\hbar$. For band 7, the peaks of the *azimuthal plot* always locate at $\theta = 90°$ for the whole observed spin region, which presents a planar rotation. Such orientations of the angular momenta for band 7 can not form the chiral geometry, which means that band 7 can not have chiral partner band. This is consistent with the present experimental observations.

4. Summary

In summary, medium- and high-spin states in the odd-A nucleus ^{81}Kr were populated using the reaction ^{82}Se(α, $5n$) at beam energies of 65 and 68 MeV. Two nearly degenerate positive-parity bands (2 and 3) with the $\pi g_{9/2}^2 \otimes \nu g_{9/2}^{-1}$ configuration and three nearly degenerate negative-parity bands (5, 6 and 7) with the $\pi g_{9/2}(p_{3/2}, f_{5/2}) \otimes \nu g_{9/2}^{-1}$ configuration have been identified. Based on the experimental features and theoretical calculations, bands 2 and 3 as well as bands 5 and 6 are interpreted as chiral doublet bands, and band 7 is interpreted as the pseudospin partner of band 5. These observations present two new chiral configurations $\pi g_{9/2}^2 \otimes \nu g_{9/2}^{-1}$ and $\pi g_{9/2}(p_{3/2}, f_{5/2}) \otimes \nu g_{9/2}^{-1}$, and the first example of pseudospin-chiral triplet bands involving the $\pi(p_{3/2}, f_{5/2})$ pseudospin doublet. In addition, the observation of the chiral doublet bands in ^{81}Kr indicates that chirality can exist not only in odd-odd nuclei but also in odd-A nuclei in the $A \approx 80$ mass region.

Declaration of competing interest

The authors declare that they have no known competing financial interests or personal relationships that could have appeared to influence the work reported in this paper.

Acknowledgements

Authors would like to thank Dr. S. Guo for discussions on the error estimation. This work is partly supported by the Major Program of Natural Science Foundation of Shandong Province (No. ZR2020ZD30), the National Natural Science Foundation of China (No. 12075137, No. 12075138, No. 11775133, No. 12035001, No. 12075006 and No. U1832211), the Natural Science Foundation of Shandong Province (No. ZR2020YQ07 and No. ZR2020QA084), the Young Scholars Program of Shandong University, Weihai and the National Research Foundation of South Africa (No. 92791, No. 92792 and No. 90741). The numerical calculations in this paper were done on the supercomputing system in the Supercomputing Center in Shandong University, Weihai. The authors thank the iThemba LABS technical staff and accelerator group for their support.

Appendix A. Supplementary material

Supplementary material related to this article can be found online at https://doi.org/10.1016/j.physletb.2022.137006.

References

[1] S. Frauendorf, J. Meng, Nucl. Phys. A 617 (1997) 131, https://doi.org/10.1016/S0375-9474(97)00004-3.
[2] J. Meng, S.Q. Zhang, J. Phys. G 37 (2010) 064025, https://doi.org/10.1088/0954-3899/37/6/064025.
[3] R.A. Bark, E.O. Lieder, R.M. Lieder, E.A. Lawrie, J.J. Lawrie, S.P. Bvumbi, N.Y. Kheswa, S.S. Ntshangase, T.E. Madiba, P.L. Masiteng, S.M. Mullins, S. Murray, P. Papka, O. Shirinda, Q.B. Chen, S.Q. Zhang, Z.H. Zhang, P.W. Zhao, C. Xu, J. Meng, D.G. Roux, Z.P. Li, J. Peng, B. Qi, S.Y. Wang, Z.G. Xiao, Int. J. Mod. Phys. E 23 (2014) 1461001, https://doi.org/10.1142/S0218301314610011.
[4] J. Meng, P.W. Zhao, Phys. Scr. 91 (2016) 053008, https://doi.org/10.1088/0031-8949/91/5/053008.
[5] A.A. Raduta, Prog. Part. Nucl. Phys. 90 (2016) 241, https://doi.org/10.1016/j.ppnp.2016.05.002.
[6] B.W. Xiong, Y.Y. Wang, At. Data Nucl. Data Tables 125 (2019) 193, https://doi.org/10.1016/j.adt.2018.05.002.
[7] J. Meng, Q.B. Chen, S.Q. Zhang, Int. J. Mod. Phys. E 23 (2014) 1430016, https://doi.org/10.1142/S0218301314300161.
[8] J. Meng, J. Peng, S.Q. Zhang, S.G. Zhou, Phys. Rev. C 73 (2006) 037303, https://doi.org/10.1103/PhysRevC.73.037303.
[9] A.D. Ayangeakaa, U. Garg, M.D. Anthony, S. Frauendorf, J.T. Matta, B.K. Nayak, D. Patel, Q.B. Chen, S.Q. Zhang, P.W. Zhao, B. Qi, J. Meng, R.V.F. Janssens, M.P. Carpenter, C.J. Chiara, F.G. Kondev, T. Lauritsen, D. Seweryniak, S. Zhu, S.S. Ghugre, R. Palit, Phys. Rev. Lett. 110 (2013) 172504, https://doi.org/10.1103/PhysRevLett.110.172504.
[10] S.Y. Wang, Chin. Phys. C 44 (2020) 112001, https://doi.org/10.1088/1674-1137/abaed2.
[11] Q.B. Chen, J. Meng, Nucl. Phys. News 30 (2020) 11, https://doi.org/10.1080/10619127.2019.1676119.
[12] I. Kuti, Q.B. Chen, J. Timár, D. Sohler, S.Q. Zhang, Z.H. Zhang, P.W. Zhao, J. Meng, K. Starosta, T. Koike, E.S. Paul, D.B. Fossan, C. Vaman, Phys. Rev. Lett. 113 (2014) 032501, https://doi.org/10.1103/PhysRevLett.113.032501.
[13] C. Liu, S.Y. Wang, R.A. Bark, S.Q. Zhang, J. Meng, B. Qi, P. Jones, S.M. Wyngaardt, J. Zhao, C. Xu, S.G. Zhou, S. Wang, D.P. Sun, L. Liu, Z.Q. Li, N.B. Zhang, H. Jia, X.Q. Li, H. Hua, Q.B. Chen, Z.G. Xiao, H.J. Li, L.H. Zhu, T.D. Bucher, T. Dinoko, J. Easton, K. Juhász, A. Kamblawe, E. Khaleel, N. Khumalo, E.A. Lawrie, J.J. Lawrie, S.N.T. Majola, S.M. Mullins, S. Murray, J. Ndayishimye, D. Negi, S.P. Noncolela, S.S. Ntshangase, B.M. Nyakó, J.N. Orce, P. Papka, J.F. Sharpey-Schafer, O. Shirinda, P. Sithole, M.A. Stankiewicz, M. Wiedeking, Phys. Rev. Lett. 116 (2016) 112501, https://doi.org/10.1103/PhysRevLett.116.112501.
[14] C.M. Petrache, B.F. Lv, A. Astier, E. Dupont, Y.K. Wang, S.Q. Zhang, P.W. Zhao, Z.X. Ren, J. Meng, P.T. Greenlees, H. Badran, D.M. Cox, T. Grahn, R. Julin, S. Juutinen, J. Konki, J. Pakarinen, P. Papadakis, J. Partanen, P. Rahkila, M. Sandzelius, J. Saren, C. Scholey, J. Sorri, S. Stolze, J. Uusitalo, B. Cederwall, Ö. Aktas, A. Ertoprak, H. Liu, S. Matta, P. Subramaniam, S. Guo, M.L. Liu, X.H. Zhou, K.L. Wang, I. Kuti, J. Timár, A. Tucholski, J. Srebrny, C. Andreoiu, Phys. Rev. C 97 (2018) 041304(R), https://doi.org/10.1103/PhysRevC.97.041304.
[15] T. Roy, G. Mukherjee, Md.A. Asgar, S. Bhattacharyya, Soumik Bhattacharya, C. Bhattacharya, S. Bhattacharya, T.K. Ghosh, K. Banerjee, Samir Kundu, T.K. Rana, P. Roy, R. Pandey, J. Meena, A. Dhal, R. Palit, S. Saha, J. Sethi, Shital Thakur, B.S. Naidu, S.V. Jadav, R. Dhonti, H. Pai, A. Goswami, Phys. Lett. B 782 (2018) 768, https://doi.org/10.1016/j.physletb.2018.06.033.
[16] B.F. Lv, C.M. Petrache, Q.B. Chen, J. Meng, A. Astier, E. Dupont, P. Greenlees, H. Badran, T. Calverley, D.M. Cox, T. Grahn, J. Hilton, R. Julin, S. Juutinen, J. Konki, J. Pakarinen, P. Papadakis, J. Partanen, P. Rahkila, P. Ruotsalainen, M. Sandzelius, J. Saren, C. Scholey, J. Sorri, S. Stolze, J. Uusitalo, B. Cederwall, A. Ertoprak, H. Liu, S. Guo, M.L. Liu, J.G. Wang, X.H. Zhou, I. Kuti, J. Timár, A. Tucholski, J. Srebrny, C. Andreoiu, Phys. Rev. C 100 (2019) 024314, https://doi.org/10.1103/PhysRevC.100.024314.
[17] S. Guo, C.M. Petrache, D. Mengoni, Y.H. Qiang, Y.P. Wang, Y.Y. Wang, J. Meng, Y.K. Wang, S.Q. Zhang, P.W. Zhao, A. Astier, J.G. Wang, H.L. Fan, E. Dupont, B.F. Lv, D. Bazzacco, A. Boso, A. Goasduff, F. Recchia, D. Testov, F. Galtarossa, G. Jaworski, D.R. Napoli, S. Riccetto, M. Siciliano, J.J. Valiente-Dobon, M.L. Liu,

G.S. Li, X.H. Zhou, Y.H. Zhang, C. Andreoiu, F.H. Garcia, K. Ortner, K. Whitmore, A. Ataç-Nyberg, T. Bäck, B. Cederwall, E.A. Lawrie, I. Kuti, D. Sohler, T. Marchlewski, J. Srebrny, A. Tucholski, Phys. Lett. B 807 (2020) 135572, https://doi.org/10.1016/j.physletb.2020.135572.

[18] C.M. Petrache, B.F. Lv, Q.B. Chen, J. Meng, A. Astier, E. Dupont, K.K. Zheng, P.T. Greenlees, H. Badran, T. Calverley, D.M. Cox, T. Grahn, J. Hilton, R. Julin, S. Juutinen, J. Konki, J. Pakarinen, P. Papadakis, J. Partanen, P. Rahkila, P. Ruotsalainen, M. Sandzelius, J. Saren, C. Scholey, J. Sorri, S. Stolze, J. Uusitalo, B. Cederwall, A. Ertoprak, H. Liu, S. Guo, J.G. Wang, X.H. Zhou, I. Kuti, J. Timár, A. Tucholski, J. Srebrny, C. Andreoiu, Eur. Phys. J. A 56 (2020) 208, https://doi.org/10.1140/epja/s10050-020-00218-5.

[19] B. Qi, H. Jia, N.B. Zhang, C. Liu, S.Y. Wang, Phys. Rev. C 88 (2013) 027302, https://doi.org/10.1103/PhysRevC.88.027302.

[20] Y.Y. Wang, S.Q. Zhang, P.W. Zhao, J. Meng, Phys. Lett. B 792 (2019) 454, https://doi.org/10.1016/j.physletb.2019.04.014.

[21] Y.Y. Wang, X.H. Wu, S.Q. Zhang, P.W. Zhao, J. Meng, Sci. Bull. 65 (2020) 2001, https://doi.org/10.1016/j.scib.2020.08.028.

[22] Joseph N. Ginocchio, Phys. Rep. 414 (2005) 165, https://doi.org/10.1016/j.physrep.2005.04.003.

[23] H. Liang, J. Meng, S.-G. Zhou, Phys. Rep. 570 (2015) 1, https://doi.org/10.1016/j.physrep.2014.12.005.

[24] H. Jia, B. Qi, C. Liu, S.Y. Wang, J. Phys. G 46 (2019) 035102, https://doi.org/10.1088/1361-6471/ab025c.

[25] S.Y. Wang, B. Qi, L. Liu, S.Q. Zhang, H. Hua, X.Q. Li, Y.Y. Chen, L.H. Zhu, J. Meng, S.M. Wyngaardt, P. Papka, T.T. Ibrahim, R.A. Bark, P. Datta, E.A. Lawrie, J.J. Lawrie, S.N.T. Majola, P.L. Masiteng, S.M. Mullins, J. Gál, G. Kalinka, J. Molnár, B.M. Nyakó, J. Timár, K. Juhász, R. Schwengner, Phys. Lett. B 703 (2011) 40, https://doi.org/10.1016/j.physletb.2011.07.055.

[26] C. Liu, S.Y. Wang, B. Qi, S. Wang, D.P. Sun, Z.Q. Li, R.A. Bark, P. Jones, J.J. Lawrie, L. Masebi, M. Wiedeking, J. Meng, S.Q. Zhang, H. Hua, X.Q. Li, C.G. Li, R. Han, S.M. Wyngaardt, B.H. Sun, L.H. Zhu, T.D. Bucher, B.V. Kheswa, K.L. Malatji, J. Ndayishimye, O. Shirinda, T. Dinoko, N. Khumalo, E.A. Lawrie, S.S. Ntshangase, Phys. Rev. C 100 (2019) 054309, https://doi.org/10.1103/PhysRevC.100.054309.

[27] X.C. Han, S.Y. Wang, B. Qi, C. Liu, S. Wang, D.P. Sun, Z.Q. Li, H. Jia, R.J. Guo, X. Xiao, L. Mu, X. Lu, Q. Wang, W.Z. Xu, H.W. Li, X.G. Wu, Y. Zheng, C.B. Li, T.X. Li, Z.Y. Huang, H.Y. Wu, D.W. Luo, Phys. Rev. C 104 (2021) 014327, https://doi.org/10.1103/PhysRevC.104.014327.

[28] R.A. Bark, M. Lipoglavšek, S.M. Maliage, S.S. Ntshangase, A. Shevchenko, J. Phys. G 31 (2005) S1747, https://doi.org/10.1088/0954-3899/31/10/066.

[29] M. Piiparinen, A. Ataç, J. Blomqvist, G.B. Hagemann, B. Herskind, R. Julin, S. Juutinen, A. Lampinen, J. Nyberg, G. Sletten, P. Tikkanen, S. Törmänen, A. Virtanen, R. Wyss, Nucl. Phys. A 605 (1996) 191, https://doi.org/10.1016/0375-9474(96)00157-1.

[30] P.M. Jones, L. Wei, F.A. Beck, P.A. Butler, T. Byrski, G. Duchêne, G. de France, F. Hannachi, G.D. Jones, B. Kharraja, Nucl. Instrum. Methods Phys. Res., Sect. A 362 (1995) 556, https://doi.org/10.1016/0168-9002(95)00246-4.

[31] C.G. Li, Q.B. Chen, S.Q. Zhang, C. Xu, H. Hua, S.Y. Wang, R.A. Bark, S.M. Wyngaardt, Z. Shi, A.C. Dai, C.G. Wang, X.Q. Li, Z.H. Li, J. Meng, F.R. Xu, Y.L. Ye, D.X. Jiang, R. Han, C.Y. Niu, Z.Q. Chen, H.Y. Wu, X. Wang, D.W. Luo, C.G. Wu, S. Wang, D.P. Sun, C. Liu, Z.Q. Li, B.H. Sun, P. Jones, L. Msebi, J.F. Sharpey-Schafer, T. Dinoko, E.A. Lawrie, S.S. Ntshangase, B.V. Kheswa, O. Shirinda, N. Khumalo, T.D. Bucher, K.L. Malatji, Phys. Rev. C 100 (2019) 044318, https://doi.org/10.1103/PhysRevC.100.044318.

[32] L. Funke, F. Dönau, J. Döring, P. Kemnitz, E. Will, G. Winter, Phys. Lett. B 120 (1983) 301, https://doi.org/10.1016/0370-2693(83)90449-5.

[33] L. Funke, J. Döring, P. Kemnitz, E. Will, G. Winter, Nucl. Phys. A 455 (1986) 206, https://doi.org/10.1016/0375-9474(86)90017-5.

[34] K. Starosta, T. Koike, C.J. Chiara, D.B. Fossan, D.R. LaFosse, A.A. Hecht, C.W. Beausang, M.A. Caprio, J.R. Cooper, R. Krücken, J.R. Novak, N.V. Zamfir, K.E. Zyromski, D.J. Hartley, D.L. Balabanski, Jing-ye Zhang, S. Frauendorf, V.I. Dimitrov, Phys. Rev. Lett. 86 (2001) 971, https://doi.org/10.1103/PhysRevLett.86.971.

[35] C. Vaman, D.B. Fossan, T. Koike, K. Starosta, Phys. Rev. Lett. 92 (2004) 032501, https://doi.org/10.1103/PhysRevLett.92.032501.

[36] G. Rainovski, E.S. Paul, H.J. Chantler, P.J. Nolan, D.G. Jenkins, R. Wadsworth, P. Raddon, A. Simons, D.B. Fossan, T. Koike, K. Starosta, C. Vaman, E. Farnea, A. Gadea, Th. Kröll, R. Isocrate, G. de Angelis, D. Curien, V.I. Dimitrov, Phys. Rev. C 68 (2003) 024318, https://doi.org/10.1103/PhysRevC.68.024318.

[37] T. Koike, K. Starosta, C. Vaman, T. Ahn, D.B. Fossan, R.M. Clark, M. Cromaz, I.Y. Lee, A.O. Macchiavelli, in: P. Fallon, R. Clark (Eds.), Frontiers of Nuclear Structure, in: AIP Conf. Proc., vol. 656, AIP, Melville, New York, 2003, p. 160.

[38] S.Y. Wang, S.Q. Zhang, B. Qi, J. Meng, Chin. Phys. Lett. 24 (2007) 664, https://doi.org/10.1088/0256-307X/24/3/021.

[39] T. Koike, K. Starosta, I. Hamamoto, Phys. Rev. Lett. 93 (2004) 172502, https://doi.org/10.1103/PhysRevLett.93.172502.

[40] G. Mukherjee, P. Joshi, R.K. Bhowmik, S.N. Roy, S. Dutta, S. Muralithar, R.P. Singh, Nucl. Phys. A 829 (2009) 137, https://doi.org/10.1016/j.nuclphysa.2009.07.016.

[41] W. Nazarewicz, Variety of shapes in the zirconium region, in: J.X. Saladin, R.A. Sorensen, C.M. Vincent (Eds.), High Spin Physics and Gamma-Soft Nuclei, World Scientific, Singapore, 1991, p. 406.

[42] Q. Xu, S.J. Zhu, J.H. Hamilton, A.V. Ramayya, J.K. Hwang, B. Qi, J. Meng, J. Peng, Y.X. Luo, J.O. Rasmussen, I.Y. Lee, S.H. Liu, K. Li, J.G. Wang, H.B. Ding, L. Gu, E.Y. Yeoh, W.C. Ma, Phys. Rev. C 78 (2008) 064301, https://doi.org/10.1103/PhysRevC.78.064301.

[43] J. Meng (Ed.), Relativistic Density Functional for Nuclear Structure, World Scientific, Singapore, 2016.

[44] J. Peng, H. Sagawa, S.Q. Zhang, J.M. Yao, Y. Zhang, J. Meng, Phys. Rev. C 77 (2008) 024309, https://doi.org/10.1103/PhysRevC.77.024309.

[45] J. Li, S.Q. Zhang, J. Meng, Phys. Rev. C 83 (2011) 037301, https://doi.org/10.1103/PhysRevC.83.037301.

[46] B. Qi, S.Q. Zhang, J. Meng, S.Y. Wang, S. Frauendorf, Phys. Lett. B 675 (2009) 175, https://doi.org/10.1016/j.physletb.2009.02.061.

[47] B. Qi, S.Q. Zhang, S.Y. Wang, J. Meng, T. Koike, Phys. Rev. C 83 (2011) 034303, https://doi.org/10.1103/PhysRevC.83.034303.

[48] W. Long, J. Meng, N. Van Giai, S.G. Zhou, Phys. Rev. C 69 (2004) 034319, https://doi.org/10.1103/PhysRevC.69.034319.

[49] P.W. Zhao, S.Q. Zhang, J. Peng, H.Z. Liang, P. Ring, J. Meng, Phys. Lett. B 699 (2011) 181, https://doi.org/10.1016/j.physletb.2011.03.068.

[50] P.W. Zhao, J. Peng, H.Z. Liang, P. Ring, J. Meng, Phys. Rev. Lett. 107 (2011) 122501, https://doi.org/10.1103/PhysRevLett.107.122501.

[51] J. Meng, J. Peng, S.Q. Zhang, P.W. Zhao, Front. Phys. 8 (2013) 55, https://doi.org/10.1007/s11467-013-0287-y.

[52] S.Y. Wang, B. Qi, S.Q. Zhang, Chin. Phys. Lett. 26 (2009) 052102, https://doi.org/10.1088/0256-307X/26/5/052102.

[53] F.Q. Chen, Q.B. Chen, Y.A. Luo, J. Meng, S.Q. Zhang, Phys. Rev. C 96 (2017) 051303(R), https://doi.org/10.1103/PhysRevC.96.051303.

[54] F.Q. Chen, J. Meng, S.Q. Zhang, Phys. Lett. B 785 (2018) 211, https://doi.org/10.1016/j.physletb.2018.08.039.

[55] Q.B. Chen, J. Meng, Phys. Rev. C 98 (2018) 031303(R), https://doi.org/10.1103/PhysRevC.98.031303.

[56] E. Streck, Q.B. Chen, N. Kaiser, Ulf-G. Meißner, Phys. Rev. C 98 (2018) 044314, https://doi.org/10.1103/PhysRevC.98.044314.

[57] J. Peng, Q.B. Chen, Phys. Lett. B 793 (2019) 303, https://doi.org/10.1016/j.physletb.2019.04.065.

[58] Y.K. Wang, F.Q. Chen, P.W. Zhao, S.Q. Zhang, J. Meng, Phys. Rev. C 99 (2019) 054303, https://doi.org/10.1103/PhysRevC.99.054303.

[59] Y.P. Wang, Y.Y. Wang, J. Meng, Phys. Rev. C 102 (2020) 024313, https://doi.org/10.1103/PhysRevC.102.024313.

[60] J. Peng, Q.B. Chen, Phys. Lett. B 806 (2020) 135489, https://doi.org/10.1016/j.physletb.2020.135489.

[61] Y.Y. Wang, S.Q. Zhang, Phys. Rev. C 102 (2020) 034303, https://doi.org/10.1103/PhysRevC.102.034303.